Deposition Mechanism of Aluminum Oxide on Quantum Dot Films at Atmospheric Pressure and Room Temperature

Valdesueiro Gonzalez, D.; Prabhu, Mahesh Krishna; Guerra-Nunez, Carlos; Sandeep, C. S Suchand; Kinge, Sachin; Siebbeles, Laurens D A; De Smet, Louis C P M; Meesters, Gabrie M H; Kreutzer, Michiel T.; Houtepen, Arjan J.

DOI
10.1021/acs.jpcc.5b11653

Publication date
2016

Document Version
Accepted author manuscript

Published in
The Journal of Physical Chemistry C

The Deposition Mechanism of Aluminium Oxide on Quantum Dot Films at Atmospheric Pressure and Room Temperature.

David Valdesueiro*[1], Mahesh Krishna Prabhu*[1], Carlos Guerra-Nunez[1,2†], C.S. Suchand Sandeep[1,3†], Sachin Kinge[1], Laurens D.A. Siebbeles[1], Louis C.P.M. de Smet[1], Gabrie M.H. Meesters[1], Michiel T. Kreutzer[1], Arjan J. Houtepen [§1], J. Ruud van Ommen[§1].

[1] Delft University of Technology, Department of Chemical Engineering, Julianalaan 136, 2628 BL, Delft, The Netherlands.

[2] EMPA, Laboratory for Mechanics of Materials and Nanostructures, Feuerwerkerstrasse 39, CH-3602 Thun, Switzerland.

[3] University of Potsdam, Institute of Physics and Astronomy, 14476, Potsdam, Germany.

§ Corresponding authors: A.J.Houtepen@tudelft.nl and J.R.vanOmmen@tudelft.nl

Telephone A.J. Houtepen: +31 (0) 15 2782157

Telephone J.R. van Ommen: +31 (0) 15 2782133

† Present address

* These authors contributed equally to this work.

ABSTRACT

Stability of quantum dot (QD) films is an issue of concern for applications in devices such as solar cells, LEDs and transistors. This paper analyzes and optimizes the passivation of such QD films using gas-phase deposition, resulting in enhanced stability. Crucially, we deposited alumina at economically attractive conditions, room temperature and atmospheric pressure, on (1,2-ethanediamine) capped PbSe QD films using an approach based on atomic layer deposition (ALD), with trimethylaluminum (TMA) and water as precursors. We performed coating experiments from 1 to 25 cycles on the QD films, finding that alumina formed from the first exposure of TMA. X-ray photoelectron spectroscopy points to the presence of oxygen-rich compounds on the bare QD films, most likely from entrapped solvent molecules during the assembly of the QD films. These oxygenated compounds and the amine groups of the organic ligands react with TMA in the first cycle, resulting in a fast growth of alumina. Using 10 cycles resulted in a QD film that was optically stable for at least 27 days. Depositing alumina at ambient conditions is preferred since the production of the QD films is also carried out at room temperature and atmospheric pressure, allowing combination of both processes in a single go.

1. INTRODUCTION

Assembled films of colloidal quantum dots (QD) have come to the fore in potential applications for photovoltaic devices [1-7] due to their size-tunable band gap and ease of processing[4, 8]. In particular, colloidal QDs exhibit efficient carrier multiplication, a process in which a high energy photon creates more than one charge carrier pair,[8-18] which can boost the efficiency in applications such as photovoltaic devices.

In optoelectronic devices, QDs are immobilized as films and separated by ligands that are bound to the QD surface. These ligands prevent sintering of the crystals [19, 20], but they also make the assembled structure more open, allowing oxygen to diffuse inside the film easily and degrade the crystals by oxidation. Good results have recently been obtained by using films of QDs capped with 1,2-ethanediamine (EDA) and 1-2,ethanedithiol (EDT) for applications in optoelectronic materials [21-24]. However, the susceptibility to air oxidation [21] in these films has been the major challenge that has frustrated the use in working devices.

This paper describes, analyzes and optimizes a passivation process for QD films. Recently, atomic layer deposition (ALD) of aluminium oxide (a.k.a. alumina; i.e., Al_2O_3), carried out at 25–75 °C and ~0.15 Torr, was used to infill and overcoat lead selenide (PbSe) QD films and stabilize them against air degradation [15, 25]. ALD of alumina involves cyclic, self-terminating, gas-phase reactions between trimethylaluminium (TMA) and an oxidizer, such as oxygen or water, to deposit thin and conformal films [26-28].

We modified this ALD process to work at economically much more attractive conditions, room temperature and atmospheric pressure. [29, 30] Typically, Al_2O_3 ALD is carried out at near vacuum to ensure the removal of unreacted species from the substrate [31-33]. Obviously,

63 avoiding vacuum would be attractive, and a room-temperature process would be completely
64 compatible with the fabrication of the QD films, which is also done under ambient conditions
65 [4]. The potential problem that requires analysis and optimization is the physisorption of
66 unreacted species on the substrate, inducing a less precise chemical vapor deposition (CVD)
67 type of growth characterized by the deposition of several layers of alumina in each cycle [30, 31,
68 34]. We show in this paper that that indeed occurs, but that this does not reduce the capacity of
69 the alumina to enhance the QD stability. Potentially, replacing the liquid precursors, i.e.,
70 water, by gaseous ones, i.e., air, could reduce the accumulation of unreacted species on the
71 QD films, providing a more precise control over the deposition of ultrathin films of alumina.
72
73 In previous work by Law and co-workers [15, 22, 25, 35], the deposition of alumina on QD films
74 successfully prevented oxidation and photo-thermal degradation, allowing direct use of such
75 films in open air. According to reference [25], the alumina acted as a matrix to prevent solid-
76 state diffusion of atoms between QDs, which also reduced the tunneling barrier for charge
77 transfer between the quantum dots and passivated surface charge traps, thereby enhancing the
78 charge mobility by one order of magnitude. However, despite the excellent performance of
79 Al_2O_3-ALD on QD films as passivating material, there is a lack of studies on the deposition
80 mechanism of alumina inside the films. Recent work done in the field has triggered interest
81 into understanding the process of alumina deposition in the pores of quantum dot films [25].
82 Parameters such as the combined effect of temperature and pressure on the deposition of
83 alumina, and the minimum amount of alumina that is required to fully protect the QD films
84 from degradation, have not been investigated yet. Also, little is known about the growth of
85 alumina in the pores of the QD film during the coating process.
86

Here we demonstrate the gas-phase deposition of alumina inside EDA capped PbSe QD films at room temperature and atmospheric pressure. The first cycles lead predominantly to infilling, i.e., the alumina grows between the QDs, and when the interstitial space between the QDs is filled, additional cycles lead to overcoating of the films, i.e., the formation of a layer of alumina on top of the QD film. For this aim, we investigated (i) the amount of alumina deposited at ambient conditions after different number of cycles, (ii) the deposition mechanism of alumina inside the films, (iii) the air-stability of QD films coated with different number of cycles, and (iv) the deposition of alumina using a diluted flow of dry air after 25 cycles and its stability under air. We observed the infilling of alumina from the first dosage of TMA, which is explained this by the reactivity of TMA molecules with hydroxyl and amine groups present in the film from the solvent and organic ligands used during the dip-coating of the QD film. Furthermore, we demonstrate that efficient infilling with Al_2O_3 at ambient pressure and room temperature is possible, significantly enhancing the speed and ease of the process. This could be easily combined with the fabrication process of the QD films, also done at ambient conditions, to develop a continuous process in which the QD films would be produced and passivated in a one-go process, using a similar technology as in spatial ALD reactors [36-38].

2. EXERIMENTAL

PbSe QD solution. To prepare the QD solution, we used the following reactants: PbO (99.999%), oleic acid (technical grade, 90%), 1-octadecene (technical grade, 90%), diphenylphosphine (98%), anhydrous 1-butanol (98%), methanol (99.8%), n-hexane (95%), acetonitrile (99.8%) and tetrachloroethylene (TCE, >99%), which were purchased from Sigma-Aldrich, trioctylphosphine (TOP, >90%) and 1,2-ethanediamine (EDA, >99.5%), purchased from Fluka, and selenium powder (200 mesh, 99.999%), purchased from Alfa Aesar. For the synthesis, 0.66 g of PbO were dissolved in a mixture of 30 mL of 1-octadecene

and 2.2 mL of oleic acid, and degassed at 100 °C for one hour under vacuum. This solution was heated to 160 °C under nitrogen atmosphere. 10.8 mL of 1 M selenium (1 M Se in trioctylphosphine mixed with 84 μL of diphenylphosphine) was then swiftly injected to the lead precursor. This mixture was allowed to react at 160 °C for 2 min to form ~6.4 nm QDs, after which it was quickly cooled by a water bath. The QDs were precipitated with butanol and methanol mixture and centrifuged at 5000 rpm for 5 minutes. The precipitate was redissolved in hexane and washed with butanol/methanol mixture once again. The QDs were then dispersed in TCE for optical absorption measurements and in hexane for film preparation. The synthesis was done in a Schlenk line under nitrogen atmosphere.

EDA in methanol solution. A 1 M solution of EDA in methanol was used to replace the original long ligands (oleic acid), to couple the QDs electronically.

Quartz substrate. The dimensions of the quartz substrates used to form the films are 25 x 10 x 1 mm. The substrates were cleaned by sonication for 5 minutes each in 5% Triton solution, deionized water and ethanol, to ensure good adhesion of the QDs to the substrate. The quartz substrates were dried in a flow of nitrogen and clamped to the mechanical arm of the dip coater.

Fabrication of QD films. We deposited the PbSe QDs on quartz substrates via layer-by-layer dip-coating in three solutions inside a N_2-purged glovebox: (i) PbSe QDs in hexane for 30 s, (ii) 1 M solution of EDA in methanol for 30 s, and (iii) rinsing solution of methanol for 30 s. The dip-coating of the substrates was repeated 20 times. The mechanical dip-coater used in the fabrication of the films was a DC Multi-8 from Nima Technology. The synthesized QD

137 films were stored in a glovebox to avoid contact with air. The fabricated films had a thickness
138 of approximately 35 nm, determined by depth profile measurements by a stylus profilometer.
139
140 **Alumina coating reactor.** The alumina coating experiments were performed in an air-tight
141 purpose-made reactor operated at atmospheric pressure and 27 °C. The operating temperature
142 was controlled by an external IR lamp and measured with a thermocouple inserted in the
143 reactor. The reactor consisted of a glass column, 42 mm of diameter and 140 mm in length,
144 with a Teflon holder inside in which the QD films were placed facing downwards, so that they
145 were exposed to the precursors during the coating. The holder has 10 slits, separated vertically
146 by 1 cm, allowing the coating of multiple samples simultaneously. The glass column and the
147 Teflon holder are fixed to the inlet and outlet connections with a ring, that sealed the reactor.
148 The reactor was provided with two valves to maintain an oxygen-free environment. The QD
149 films are loaded into the reactor inside a glovebox, to avoid that the QD are exposed to air,
150 and then transported to the coating setup, in which we connected the reactor to the inlet of the
151 precursors. A sintered stainless steel SIKA-R 20 AX distributor plate with a pore size of 37
152 μm was used to homogeneously distribute the flow of precursors inside the reactor. The off-
153 gas from the reactor is taken to a series of bubblers filled with Kaydol oil, to trap unreacted
154 molecules of the precursors and the by-products of the coating reaction. The precursor
155 bubblers, the glass column and the washing bubblers are placed inside a nitrogen-blanketing
156 cabinet as a safety measure for working with TMA. The cabinet is operated at an O_2
157 concentration below 6%.
158
159 **Alumina coating precursors.** Semiconductor grade trimethylaluminium, purchased from
160 Akzo Nobel, distilled water and synthetic air were used as precursors, while pressurized N_2
161 grade 5.0 was used to transport the precursors to the reactor, and to purge it after each

reaction. TMA and water were placed in a 600 mL WW-600 stainless steel bubbler and kept at 30 °C during the coating experiments. To have a comparable concentration of oxygen to the equivalent experiments with water, we mixed a flow of 0.5 L/min of N_2 with 0.1 L/min of dry air. Some of the experiments were done using H_2O as second precursor, and few others using synthetic air. A fixed gas flow of 0.6 L/min was chosen for all the experiments performed.

Alumina coating experiments. We used dosing times per cycle of 15 s – 5 min – 15 s – 5 min for the dosing sequence TMA – N_2 – H_2O/synthetic air – N_2 to coat two QD films, which were placed at the same height of the holder in all the experiments. The same dosing times were used in all the coating experiments. We performed coating experiments at 27 °C and 1 bar with different number of cycles, i.e., 1, 3, 5, 8, and 25 cycles, using three different substrates: PbSe QD films prepared with EDA-methanol solution, PbSe QD films prepared using EDA-acetonitrile solution, and a dodecanethiol self-assembled monolayer on a gold-coated substrate. To study the air-stability, we prepared other Al_2O_3-coated films with 1, 10 and 25 cycles, using the same dosing and purging times, i.e. 15 s – 5 min – 15 s – 5 min. We also performed a 90-cycle experiment on a PbSe QD film using shorter dosing times, i.e., 0.5 s – 5 min – 0.5 s – 5 min. The total amount of both precursors dosed during the 90 shorter cycles would be equivalent to the amount dosed during 3 cycles using the same dosing times as in the rest of the samples, i.e., 15 s – 5 min – 15 s – 5 min. For this reason, we refer to this 90-shorter-cycle sample as the sample coated with "*3 equivalent cycles*" (Figure 8b), in order to compare the air-stability with the rest of the coated QD films.

Characterization of the deposition of Al_2O_3. To study the deposition of alumina, we transferred the coated samples from the detachable air-tight coating reactor to the X-ray photoelectron spectrometer (XPS) through a glovebox antechamber (under N_2 atmosphere)

attached to the XPS to ensure the samples were not oxidized before the analysis. We measured the concentration depth profile of the different elements with a Thermo Scientific X-ray photoelectron spectrometer K-Alpha, equipped with a monochromatic Al Kα radiation source and a pass energy of 100 eV for the survey scan, and ion-beam etching unit. The XPS device, which operates at ultrahigh vacuum, is equipped with an etching unit, which uses Ar^+ ions with energy of 1000 eV and a raster size of 2 mm, to remove layers of the QD films with an etching rate of 0.5 nm/s (Supporting Information SI I). We used the combination of the XPS and etching unit to measure the concentration depth profile of the coated substrates. During the XPS analysis, the spectra of the elements was charge-corrected with the adventitious carbon peak at 284.8 eV. We used the software Thermo Avantage 5.913 and Gaussian curves to deconvolute the peaks. During the XPS measurements, we used the flood gun to compensate for the positive charge. We used a microtome to prepare a slice of one alumina-coated QD film and examine it under a Tecnai F20 Transmission Electron Microscope (TEM). We measured the film thickness of the alumina overcoat in 130 points from nine TEM images to determine the mean value of the alumina film and the standard deviation.

Characterization of the air stability of the coated QD films. The alumina-coated and uncoated QD films were exposed to air at 80 °C and UV light, and their optical absorption spectra were measured using a Perkin-Elmer Lambda 900 spectrophotometer, equipped with an integrating sphere. The position of the maximum peak of the band gap indicates the stability of the QD crystals, since the band gap absorption peak blue shifts and broadens in the case of oxidation of the PbSe QD films. We measured the absorption spectrum of all the uncoated QD films before the coating experiments. The coated QD films were exposed to air, and the optical absorption was measured periodically, from 1 to 63 days.

Preparation of the dodecanethiol self-assembled monolayer. We used the following solutions to prepare the self-assembled monolayer (SAM): dodecanethiol (>99.5%), ethanol (>99%) and nitric acid (63%), purchased from Sigma Aldrich. As substrate, we used 10 mm x 10 mm x 1 mm glass plates, sputter-coated with 200 nm thick gold layer (purchased from SSens BV, The Netherlands). The gold-coated substrates were washed in a 2% nitric acid solution for 5 min and then rinsed with ethanol and dried under nitrogen. The plates were then immersed in a 1 M solution of dodecanethiol in ethanol for 18 h. After that, the plates were taken out, washed with pure ethanol and dried under a nitrogen atmosphere.

3. RESULTS AND DISCUSSIONS

In this work, we infilled and overcoated QD films with alumina in the gas phase at atmospheric pressure and room temperature. We used PbSe QD films with a thickness of 35 nm, measured with a step-profilometer, consisting of 6 nm QDs separated by EDA organic ligands. In each experiment, two films were placed in the reactor holder at the same height. Alumina ALD is typically carried out using TMA and water as precursors according to the general reaction mechanism consisting of two subsequent reactions, in which || denotes the surface species [26].

Reaction A: $||– Al – OH + Al(CH_3)_3 \rightarrow ||– Al – O – Al(CH_3)_2 + CH_4$

Reaction B: $||– Al – O – Al(CH_3)_2 + 2\ H_2O \rightarrow ||– Al – O – Al – (OH)_2 + 2\ CH_4$

In reaction A of the first cycle, functional groups are needed to react with the precursor molecules and initiate the deposition. These active sites can be any group that readily reacts with TMA molecules, such as hydroxyl and amine groups [26, 39]. During the first cycles, both

precursors can diffuse through the voids of the QD films, depositing alumina inside the film, i.e., the infilling stage. By increasing the number of cycles, the voids would get fully infilled and the precursors react on the surface of the QD film, creating an overcoating (Figure 1).

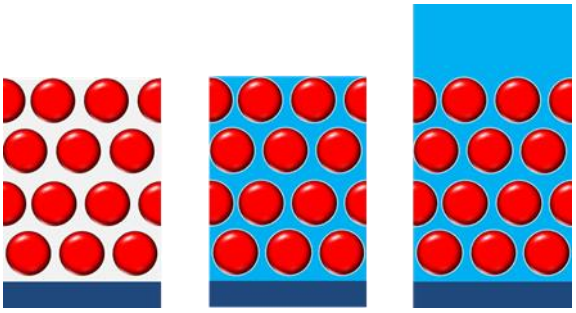

Figure 1. Cartoon showing (from left to right) an uncoated, an infilled and overcoated QD film (red spheres) with alumina (blue matrix).

Deposition of Al_2O_3 using water as precursor. We performed 1, 3, 5, 8 (Figure 2) and 25 cycles (Figure 3), at 27 °C and 1 bar, to study the growth of alumina inside the PbSe QD films. In the concentration depth profile, we observed the evolution of the intensity of the different peaks of Pb4f and Se3d belonging to the QDs, Al2p coming from the deposited alumina, C1s from the EDA ligands, Si2p from the quartz substrate, and O1s from both deposited alumina and quartz substrate.

During the initial coating cycles, i.e., 1 and 3 cycles (Figure 2a and 2b), both TMA and water penetrated all the way to the wafer through the pore network between the QDs and deposited as alumina in the entire film. This is clearly seen from the atomic percentages of Pb, Se and Al in Figure 2a, that remain more or less constant with the increased etching of the assembled film, all the way down to the quartz substrate. Similarly, the depth profiles of the films coated with 5 and 8 cycles (Figure 2c and 2d) show that alumina is deposited down to the quartz substrate. Figures 2b-d show the growth of the overcoating as the atomic percentage of

aluminium and oxygen increases at the surface with increasing number of cycles. Furthermore, we can observe the concentration of Al and O throughout the PbSe QD film remained relatively unchanged from 1-8 cycles. This suggests that the pore network is closed during the first 1-3 cycles and subsequent cycles will only deposit as an overcoating layer.

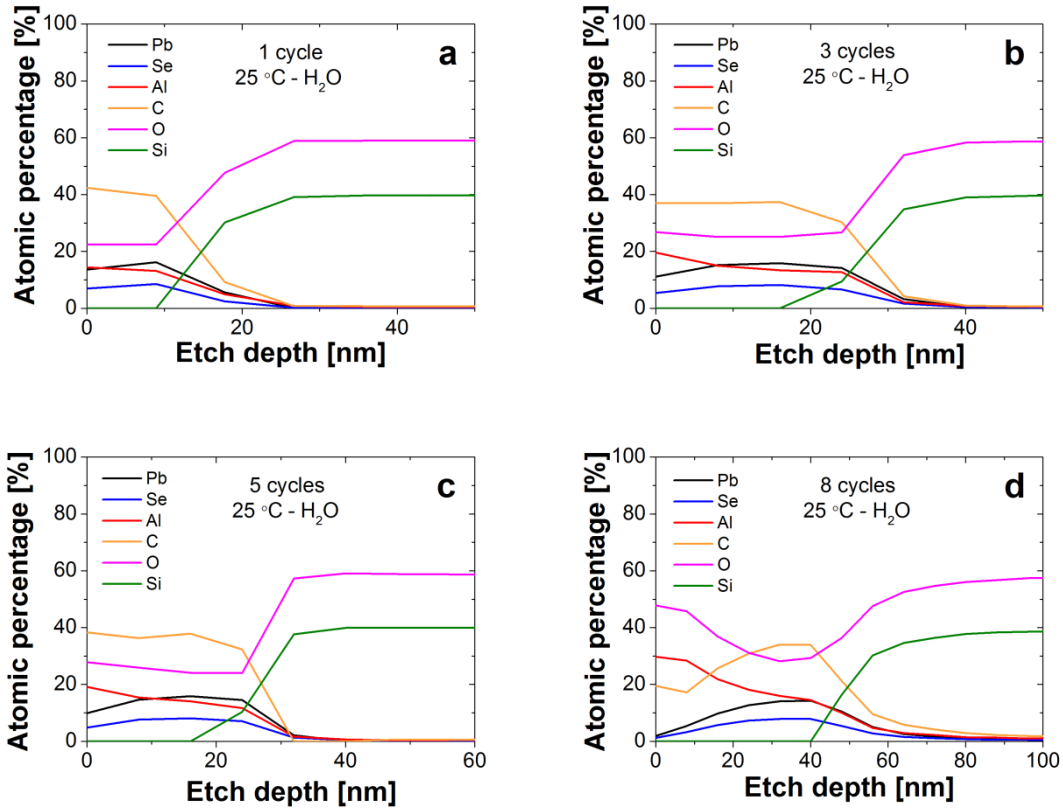

Figure 2. XPS concentration depth profile of the PbSe QD films coated with alumina after **(a)** 1 cycle, **(b)** 3 cycles, **(c)** 5 cycles and **(d)** 8 coating cycles. The depth profiles were obtained by etching the QD films with Ar^+ ion beam.

Figure 3a shows the alumina overcoating formed in the sample coated with 25 cycles, since only the signals of Al and O are present during the first tenths of nanometers in the concentration depth profile. The Al:O ratio in the overcoating is around 1.5 as expected for Al_2O_3. Additionally, the overcoating of this sample was partially etched and the XPS spectra measured, showing that the O1s and Al2p peaks are composed by Al-OH and Al_2O_3 peaks after deconvolution (Supporting Information SI II). This indicates the low presence of

impurities and unreacted methyl groups within the alumina overcoating. This overcoating can be clearly seen in the cross sectional TEM image of a 25-cycle sample (Figure 3b). Note that the XPS profile and TEM image in Figure 3 do not correspond to the same sample, but to two different batches.

Carbon was also detected on the surface and within the alumina overcoating on the 25-cycle QD film (Figure 3a). The carbon at the surface is due to adventitious carbon from environmental contamination. The carbon signal within the overcoating (< 3%) probably originated from unreacted methyl groups from the TMA molecules. Once the alumina overcoat is etched away and the PbSe/Al_2O_3 film is measured, the atomic percentage of C increased again, most likely from the combination of EDA ligands , residues from the wet chemistry process and possibly from unreacted methyl groups as observed in the overcoating. In the XPS spectra of the films coated with 1, 3, 5 and 8 cycles (Figure 2), C1s was also detected in a similar atomic percentage. This indicates that the alumina does not completely replace the organic ligands, but likely deposits around them and on the surface of the QD crystals. Based on these results, we conclude that alumina is deposited inside the QD film during the first cycles, and subsequent cycles will form an overcoating.

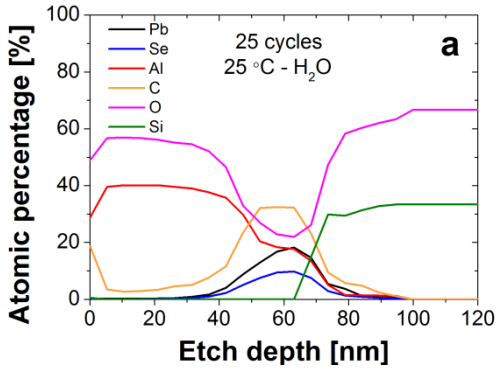

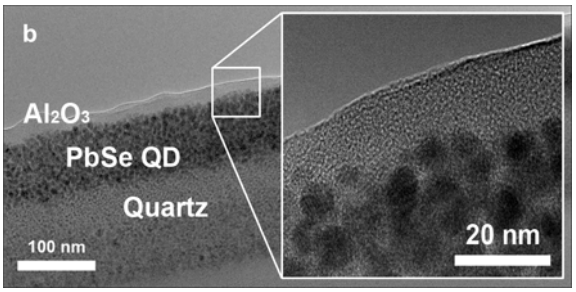

Figure 3. (a) XPS depth profile of the QD sample coated with 25 cycles of alumina. **(b)** Cross-section TEM image of the 25-cycle QD film, in which the alumina overcoating is visible.

To gain more insight into the deposition process, we first calculated a growth per cycle (GPC) of alumina during the infilling, considering that the alumina only deposits on the surface of the QD crystals. And secondly, we studied the deposition of alumina on different substrates to study the reaction of the precursors inside the QD films and define a reaction mechanism. For that, we dosed TMA to different substrates, i.e., a QD film prepared with methanol as solvent, a QD film prepared using acetonitrile as solvent, and a substrate covered with a dodecanethiol self-assembled monolayer.

Estimation of the growth per cycle of Al_2O_3. To calculate the amount of alumina deposited in each cycle, we modelled the PbSe QD film as an array of closed pack monodispersed spheres, with a particle diameter (d_P) of 6.4 nm, separated by 1,2-ethanediamine organic ligands. We assumed that alumina was only deposited on the surface of the QD crystals. The atomic ratio between Pb and Se atoms in a QD is, on average, 1.9:1 according to the XPS results (Figure 2). An excess of Pb is common for PbSe QDs [40, 41], although we note that the ratio observed here is higher than usually reported. We used the atomic ratio of Pb and Al in the film coated with 1 cycle (Figure 2a), to calculate the number of atoms of aluminium per QD. Using the molecular mass of Al_2O_3 and its density [32], we calculate that 0.6 nm of alumina

316 was deposited in the first cycle (See Supporting Information III for calculation details).
317 Considering that the theoretical size of an Al_2O_3 monolayer is about 0.38 nm [31], we estimate
318 that 1.5 monolayers of alumina were deposited per cycle during the infilling of the QD films.
319 However, this value of the GPC could be lower if we consider that alumina could deposit also
320 around the organic ligands.
321
322 **Study of the deposition mechanism of Al_2O_3.** The GPC of alumina during infilling and the
323 relatively large overcoating-film thickness measured from TEM (Figure 3b) indicates that the
324 deposition of alumina is faster than expected for ALD experiments, i.e., 0.1-0.2 nm per cycle.
325 Working at ambient conditions can involve a CVD-type of growth due to accumulation of
326 unreacted precursor molecules on the substrate [30]. However, we found a high deposition of
327 alumina during the first cycle, where no unreacted water was present. To explain this, we
328 investigated three possible mechanisms. First, we studied whether TMA molecules could
329 physisorb on the ligands by exposing a dodecanethiol self-assembled monolayer film to TMA.
330 Secondly, we investigated whether there are any remaining solvent molecules, used in the dip-
331 coating process, entrapped in the QD film which may act as active sites. For this purpose, we
332 measured the concentration depth profile of uncoated QD films prepared with different
333 solvents during dip-coating. And finally, we investigated whether the amine groups from the
334 EDA organic ligands could act as active sites and react with TMA molecules.
335
336 **Study of the reaction of TMA on a dodecanethiol SAM.** We used a self-assembled
337 monolayer of dodecanethiol on a gold substrate to study whether TMA molecules would
338 physisorb on the organic ligands. If true, this would result in a faster deposition of alumina.
339 We prepared a dodecanethiol SAM , and loaded it into the coating reactor inside a glovebox
340 under N_2 atmosphere to prevent contact with air and humidity, and carried out a half-coating

cycle, i.e., we just exposed the film to TMA. We measured the atomic percentages on the surface of the exposed SAM (Figure 4), finding a small amount of aluminium. In case TMA molecules would physisorb on carbon groups, we would have found a larger amount of aluminium with XPS. This result suggests that TMA does not physisorb on carbon groups, thus it is unlikely that it would on the EDA organic ligands with similar methyl groups. We calculated that a full monolayer of physisorbed TMA would produce an atomic percentage of about 3.5%, while in Figure 4 it is only ~ 0.3% (Supporting Information SI IV). This is an order of magnitude difference; of course, a SAM is different from the 3D complex structure of ligands in the assembled QD film, but the results obtained here are convincing enough to, as a first approximation, rule out physisorption of TMA in the ligand shell.

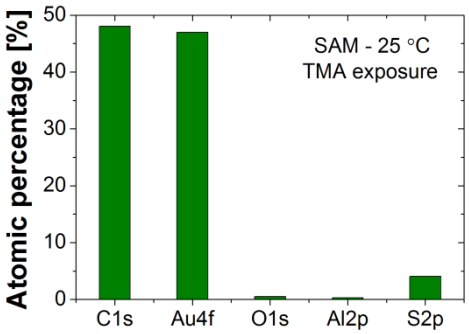

Figure 4. Atomic **c**oncentrations from XPS on the surface of the SAM after being exposed to TMA.

XPS depth profile of an uncoated QD film. We measured the concentration depth profile of the uncoated QD film to study the presence of remaining molecules from the solvents used in the dip-coating process (Figure 5). As expected, no Al traces were detected; however, O1s signals were observed. This may point to the presence of oxygenated compounds that could possibly react with TMA molecules during the first cycle causing a fast deposition of alumina.

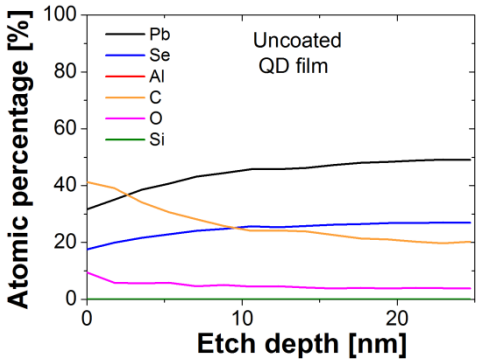

Figure 5. XPS concentration depth profile of an uncoated QD film.

To determine the nature of the source of oxygen, we studied the spectra of the elements detected by XPS after etching 7 nm of the PbSe QD film (Figure 6). At this depth, N1s signals were observed, which can be attributed to the NH bonds present in the EDA organic ligands, and a Se Auger peak, both in the same range of binding energies (Figure 6a). The intense peak at 284.8 eV (Figure 6b) indicates the presence of C-C bonds [42-45]. The peaks at 286.1 and 288.7 eV are attributed to C atoms bound to electronegative atoms [45-47], such as –COOH or –COH (Figure 6b). These results are consistent with the presence of a peak at 533 eV, which is typical of –OH groups (Figure 6c). The acid groups may originate from the oleic acid used to prepare the colloidal solution of PbSe QD crystals, while the observed alcohol features could come from the methanol used during the fabrication of the QD films via dip-coating. To conclude this part, the XPS spectra give strong evidence of the presence of oxygen-rich compounds and –NH bonds, which could react with TMA molecules during the first cycle, causing a fast deposition of alumina.

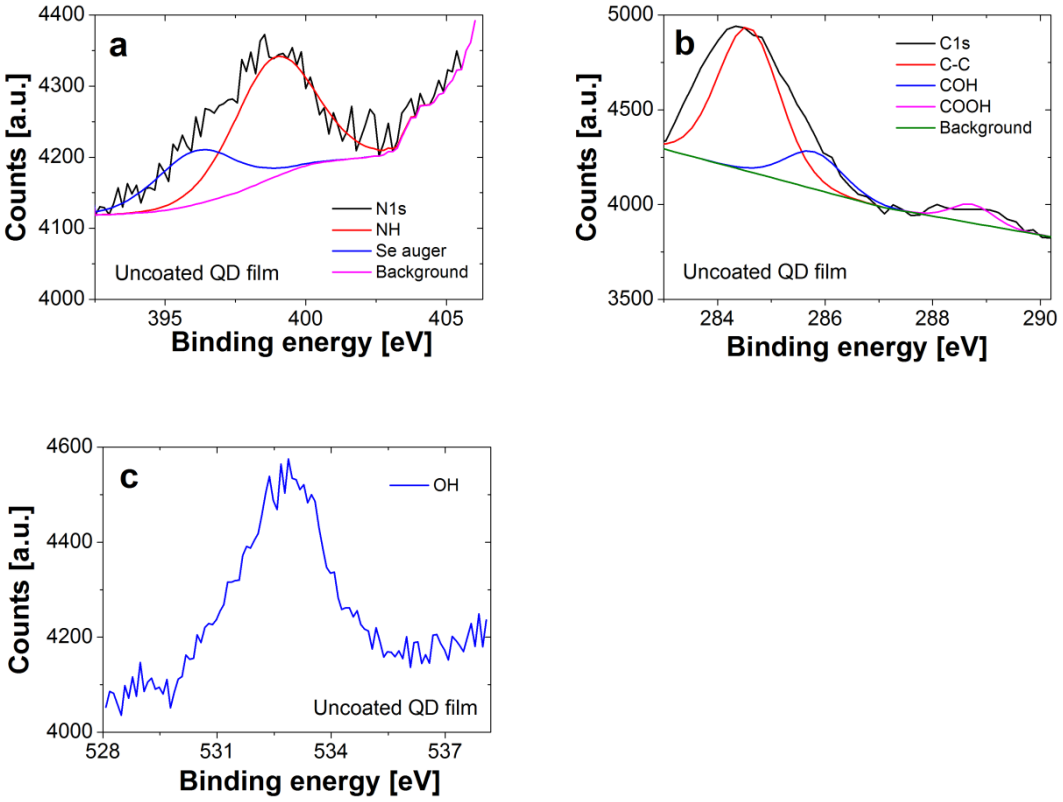

Figure 6. XPS spectra of the different elements found in an uncoated PbSe QD film, at an etch-depth of approximately 7 nm. **(a)** Elements corresponding to the QD film, such as nitrogen and selenium. **(b)** C1s region spectrum, showing different contributions of carbon, including alcohol and acid bonds, and **(c)** hydroxyl groups.

To investigate the possible role of the solvent used during dip-coating, we exposed three QD films, prepared with three different processes, to a single pulse of TMA without completing the cycle with water. These three samples were: (i) QD film prepared using a solution of EDA in methanol (Fig. 7a), exactly the same as the QD films that were coated with alumina; (ii) QD film prepared exactly the same way as the previous one, but drying it after the fabrication for 24h in a vacuum chamber at room temperature (Fig. 7b); (iii) QD film prepared using a solution of the EDA ligands in acetonitrile instead of methanol (Fig. 7c). In this way, we aimed to reduce the presence of oxygenated compounds inside the QD films and study the reaction between TMA molecules and nitrogen-based functional groups, such as $–NH_2$ from

the EDA ligands and –CN from the acetonitrile. In Fig 7 we show the concentration depth profiles after one exposure to TMA for the different fabrication processes. In the sample that was not dried (Fig. 7a), hardly any nitrogen was detected. We found, however, that by decreasing the exposure time to the beam nitrogen could be detected. Therefore, we reduced the exposure time to the ion beam, resulting in the positive detection of nitrogen (Fig. 7b and 7c). The rest of the elements showed similar profiles between the samples with no treatment and drying post-treatment (Fig. 7a and 7b). Oxygen was detected in the sample prepared with acetonitrile (Fig. 7c). One would expect this sample to contain considerably less oxygen than the samples prepared with methanol. This suggests that the oxygen might come from the remaining oleate on the QD surface, as it is known that protic solvents such as methanol are more efficient in removing oleate [48], which also explains why the QD film prepared with acetonitrile is thinner than the ones prepared with methanol.

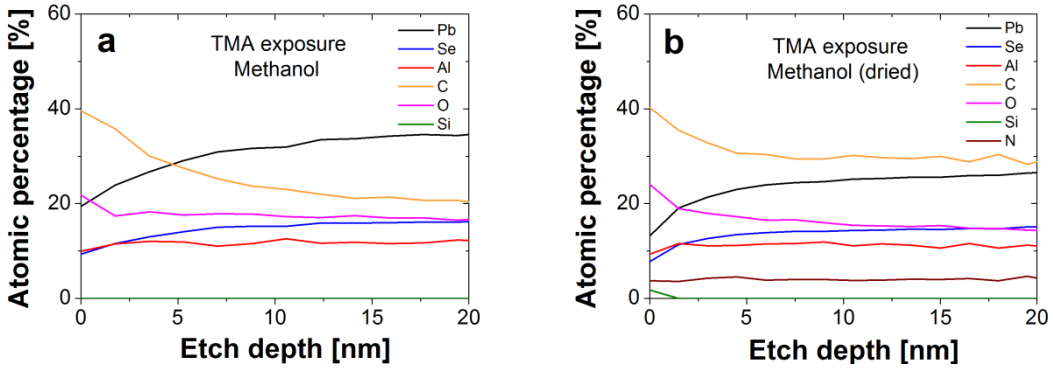

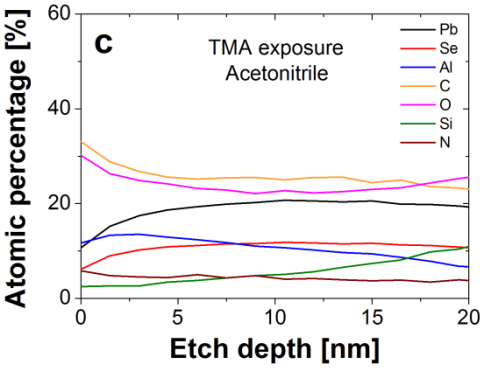

Figure 7. XPS depth profiles after dosing one pulse of TMA to **(a)** a QD film prepared with a solution of EDA ligands in methanol, **(b)** a QD film prepared with a solution of EDA ligands in methanol and dried for 24h under vacuum, and **(c)** a QD film prepared with a solution of EDA ligands in acetonitrile.

Reaction between TMA and amine groups. As the third possibility, we could explain the high deposition of alumina by the reaction between TMA molecules and the amine groups of the EDA organic ligands. According to the general scheme of Al_2O_3-ALD, TMA would react with hydroxyl groups to form alumina. However, it does not necessarily have to begin with OH groups. Al_2O_3 has been deposited on boron nitride (BN) hexagonal platelet-like particles via ALD [49]. BN surfaces contain both hydroxyl and amine functional groups [50-52], which would react with TMA molecules. In addition, ammonia has been used as second precursor in ALD, to deposit aluminium nitride (AlN) [27, 39], proving the reactivity between TMA and amine groups. Therefore, the amine groups from the EDA ligands could act as active sites where TMA can chemisorb during the first cycle. In the second cycle, after the first exposure of water, only hydroxyl groups would be available for reaction, since amine groups cannot be regenerated by using water as second precursor.

We conclude that the fast deposition of alumina during the first cycle cannot be explained by one single cause, but rather as the contribution of the hydroxyl and amine active sites present in the uncoated film and the large excess of precursor molecules, which results in a CVD-type of deposition. We note that, while unexpected, this allows very easy and rapid infilling of these QD films by a single exposure to TMA at room temperature and atmospheric pressure.

Study of the air stability of Al_2O_3-coated QD films. We investigated the air stability of the QD films coated with different film thickness of Al_2O_3. In this study, we used a solution of EDA in methanol to prepare the QD films. We evaluated four samples: an uncoated QD film, a film coated at 27 °C with an amount of alumina equivalent to 3 cycles, a film coated with 10 cycles at 70 °C, and a film coated with 25 cycles at 27 °C. The uncoated and coated QD films were exposed to air for a period of time. Subsequently, these films were placed inside an oven exposed to air at 80 °C for another period of time, similar to the accelerated tests for photovoltaic devices [53].

We measured the optical absorption spectra of each film periodically, and compared them with the spectra of each film before the alumina coatings (shown as the *0 days* curves). We assessed the stability of the QD films by measuring the position of the first exciton peak in the optical absorption spectra, which corresponds to the band gap of the QD film. Upon oxidation, the absorption peak exhibits a blue shift and broadening due to the oxidation of the QD, which results from an effective reduction of the QD size, as seen for the uncoated QD film (Figure 8a). The quick oxidation of the QD agrees with previous studies [21]. We found that 3 cycles does not deposit enough amount of alumina to fully protect the QD film from oxidation (Figure 8b). However, the films coated with 10 and 25 cycles at 70 °C and 27 °C, respectively, were stable upon air exposure during the measurement period (Figure 8c). The film with 10 cycles was coated at 70 °C rather than 27 °C as it was done with the other films. We predict that at 70 °C, less amount of alumina would be deposited since there would be a more efficient desorption of the unreacted molecules than at room temperature. That means that we could safely assume that 10 cycles at 27 °C would also stabilize the QD film, and possibly with lower number of cycles. As expected, 25 cycles at 27 °C provided full protection against oxidation of the QD film (Figure 8d), for at least a measurement period of

63 days. In addition, the XPS spectra of the etched QD film coated with 25 cycles showed that the PbSe QDS did not oxide during the coating process (Supporting Information SI V).

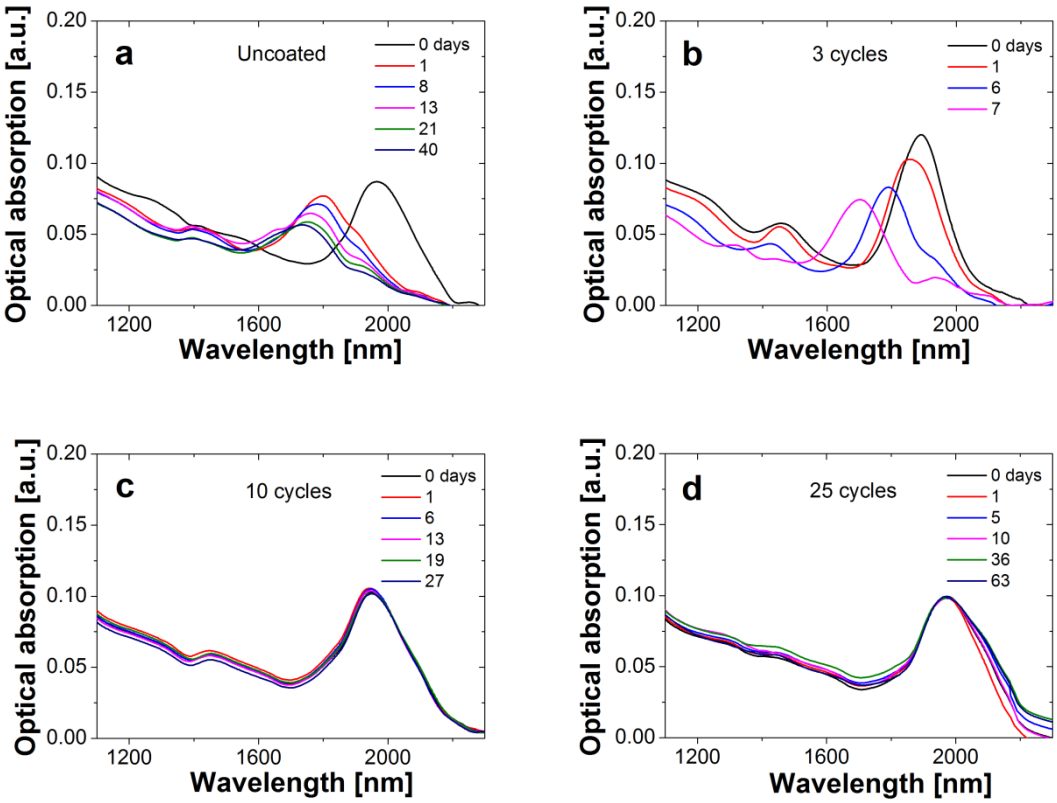

Figure 8. Optical absorption spectra of **(a)** uncoated QD film, **(b)** QD coated at 27 °C with an amount of alumina equivalent to 3 cycles, **(c)** QD coated with 10 cycles at 70 °C, and **(d)** QD coated with 25 cycles at 27 °C, measured periodically after exposure to air at 80 °C and UV light.

Study of the deposition of Al_2O_3 using synthetic air as co-reactant. To complete this study, we used an alternative second precursor, a diluted flow of air instead of water, to investigate whether we could reduce the deposition rate of alumina and get closer to the ALD growth, since it is easier to remove the excess of oxygen molecules compared to water molecules. We performed 25 cycles, and measured the concentration profile with XPS (Figure 9a). It seemed

that both infilling and overcoating occurred, although in this case the overcoating thickness is thinner than the one with water (Figure 3a). Water has a strong tendency to adsorb on the surface, especially at room temperature and atmospheric pressure [54]. However, we found that the QD film showed signs of oxidation during the coating with oxygen (Figure 9b); this was not observed when using water as co-reactant. We performed an additional coating experiment with 1 cycle, using synthetic air as second precursor, to study the oxidation of the QDs. We measured the optical absorption of the films before and after coating them with 1 and 25 cycles, and found a blue shift of the band gap. The shift of the band gap is similar for both 1- and 25-cycle QD films, indicating that the crystals mainly oxidized during the first cycle. The band gap shifted to a wavelength of 1800 nm, very similar to the shift of the uncoated QD film after air exposure (Figure 9b), which shifted to 1750 nm approximately. That indicates that using a synthetic stream of air as second precursor, even with a low concentration of oxygen, degraded the QD crystals, and that air is not an adequate oxidizer for the deposition of Al_2O_3 on QD films.

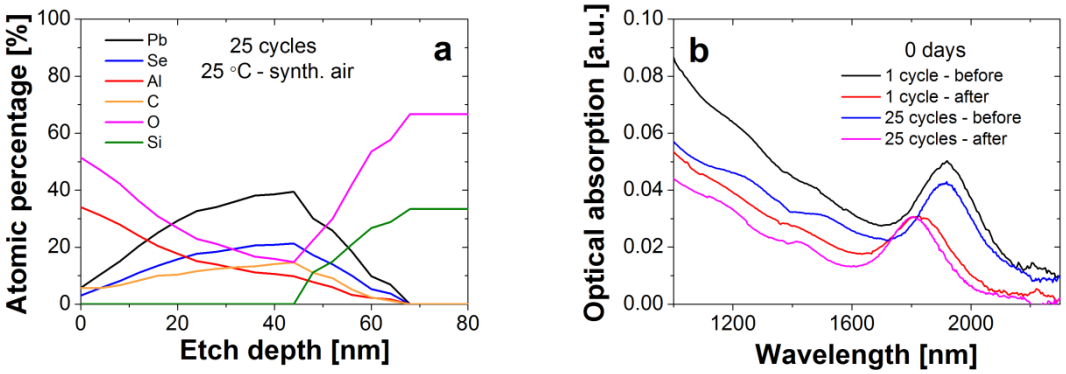

Figure 9. (a) XPS depth profile of PbSe QD film coated with 25 cycles of alumina, using synthetic air as oxidizer. **(b)** Optical absorption spectra of QD films coated with 1 and 25 cycles of alumina when using synthetic air as oxidizer.

CONCLUSIONS

We deposited alumina on PbSe QD films at room temperature and atmospheric pressure, using an ALD-like approach. During the first cycles, the alumina infilled the voids of the QD films, and after several cycles, there was a transition at which an alumina overcoating was formed. The combination of infilling and overcoating for a number of cycles between 3 and 10 effectively passivated the QD film, which did not show any oxidation after an exposure to air at 80 °C and UV light for a maximum time tested of 27 days. We calculated that during the first cycle, we deposited about 1.5 monolayers of alumina on the QD crystals. We think that this fast growth is due to the combination of the dosage of excess of precursors, and the presence of hydroxyl and amine groups inside the film, which act as active sites. Having a higher deposition rate of alumina at atmospheric pressure and 27 °C, was beneficial to infill and overcoat the QD films faster to stabilize the samples against oxidation. Finally, we deposited alumina using synthetic air as second precursor, instead of water, to reduce the physisorption of water molecules that produced the rapid growth of alumina, obtaining a thinner overcoating than the one deposited with water. However, the PbSe crystals degraded even during the first exposure to synthetic air. This work shows that depositing alumina on QD films at atmospheric pressure and room temperature gives results that are similar to those obtained at lower pressures. Working at ambient conditions facilitates the processing of QD films, since less equipment is required, and can be coupled directly to the fabrication of QD films, which is also done at atmospheric pressure and room temperature.

SUPPORTING INFORMATION

Explanation of the estimation of the growth of the deposited alumina coating on QD and SAM films from XPS measurements. Determination of the presence of impurities in the alumina overcoating, and evaluation of the oxidation state of the QDs after the deposition of alumina.

ACKNOWLEDGEMENTS

The authors would like to thank John Suijkerbuijk for the technical support in the XPS measurements. D.V., G.M.H.M., M.T.K. and J.R.vO. were supported financially by the European Union Seventh Framework Program FP7/2007-2013 under grant agreement no. 264722. D.V., G.M.H.M., M.T.K. and J.R.vO. acknowledge Royal DSM for partly funding this research.

REFERENCES

1. Ip, A. H.; Thon, S. M.; Hoogland, S.; Voznyy, O.; Zhitomirsky, D.; Debnath, R.; Levina, L.; Rollny, L. R.; Carey, G. H.; Fischer, A.; Kemp, K. W.; Kramer, I. J.; Ning, Z.; Labelle, A. J.; Chou, K. W.; Amassian, A.; Sargent, E. H., Hybrid passivated colloidal quantum dot solids. *Nat Nano* **2012,** 7, (9), 577-582.
2. Nozik, A. J.; Beard, M. C.; Luther, J. M.; Law, M.; Ellingson, R. J.; Johnson, J. C., Semiconductor quantum dots and quantum dot arrays and applications of multiple exciton generation to third-generation photovoltaic solar cells. *Chemical Reviews* **2010,** 110, (11), 6873-6890.
3. Hillhouse, H. W.; Beard, M. C., Solar cells from colloidal nanocrystals: Fundamentals, materials, devices, and economics. *Current Opinion in Colloid & Interface Science* **2009,** 14, (4), 245-259.
4. Tang, J.; Kemp, K. W.; Hoogland, S.; Jeong, K. S.; Liu, H.; Levina, L.; Furukawa, M.; Wang, X.; Debnath, R.; Cha, D.; Chou, K. W.; Fischer, A.; Amassian, A.; Asbury, J. B.; Sargent, E. H., Colloidal-quantum-dot photovoltaics using atomic-ligand passivation. *Nat Mater* **2011,** 10, (10), 765-771.
5. Lee, H. J.; Yum, J. H.; Leventis, H. C.; Zakeeruddin, S. M.; Haque, S. A.; Chen, P.; Seok, S. I.; Grätzel, M.; Nazeeruddin, M. K., CdSe quantum dot-sensitized solar cells exceeding efficiency 1% at full-sun intensity. *Journal of Physical Chemistry C* **2008,** 112, (30), 11600-11608.
6. Sandeep, C. S. S.; Cate, S. T.; Schins, J. M.; Savenije, T. J.; Liu, Y.; Law, M.; Kinge, S.; Houtepen, A. J.; Siebbeles, L. D. A., High charge-carrier mobility enables exploitation of carrier multiplication in quantum-dot films. *Nature Communications* **2013,** 4.
7. Luther, J. M.; Law, M.; Beard, M. C.; Song, Q.; Reese, M. O.; Ellingson, R. J.; Nozik, A. J., Schottky Solar Cells Based on Colloidal Nanocrystal Films. *Nano Letters* **2008,** 8, (10), 3488-3492.
8. Nordell, K. J.; Boatman, E. M.; Lisensky, G. C., A Safer, Easier, Faster Synthesis for CdSe Quantum Dot Nanocrystals. *Journal of Chemical Education* **2005,** 82, (11), 1697.
9. Beard, M. C., Multiple Exciton Generation in Semiconductor Quantum Dots. *J. Phys. Chem. Lett.* **2011,** 2, 1282-1288.
10. Beard, M. C.; Luther, J. M.; Semonin, O. E.; Nozik, A. J., Third generation photovoltaics based on multiple exciton generation in quantum confined semiconductors. *Acc Chem Res* **2013,** 46, (6), 1252-60.
11. Nair, G. C., L. Y.; Geyer, S. M.; Bawendi, M. G. , Perspective on the Prospects of a Carrier Multiplication Nanocrystal Solar Cell. *Nano Lett.* **2011**, (11), 2145-2151.
12. Beard, M. C. E., R. J. , Multiple Exciton Generation in Semiconductor Nanocrystals: Toward Efficient Solar Energy Conversion. *Laser Photonics Rev.* **2008**, (2), 377-399.
13. McGuire, J. A. J., J.; Pietryga, J. M.; Schaller, R. D.; Klimov, V. I. , New Aspects of Carrier Multiplication in Semiconductor Nanocrystals. . *Acc. Chem. Res.* **2008**, (41), 1810-1819.
14. Nozik, A. J., Multiple Exciton Generation in Semiconductor Quantum Dots. *Chem. Phys. Lett.* **2008**, (457), 3-11.
15. Ten Cate, S.; Liu, Y.; Suchand Sandeep, C. S.; Kinge, S.; Houtepen, A. J.; Savenije, T. J.; Schins, J. M.; Law, M.; Siebbeles, L. D. A., Activating carrier multiplication in PbSe quantum dot solids by infilling with atomic layer deposition. *Journal of Physical Chemistry Letters* **2013,** 4, (11), 1766-1770.
16. Aerts, M.; Suchand Sandeep, C. S.; Gao, Y.; Savenije, T. J.; Schins, J. M.; Houtepen, A. J.; Kinge, S.; Siebbeles, L. D. A., Free charges produced by carrier multiplication in strongly coupled pbse quantum dot films. *Nano Letters* **2011,** 11, (10), 4485-4489.

17. Gao, Y.; Talgorn, E.; Aerts, M.; Trinh, M. T.; Schins, J. M.; Houtepen, A. J.; Siebbeles, L. D. A., Enhanced hot-carrier cooling and ultrafast spectral diffusion in strongly coupled PbSe quantum-dot solids. *Nano Letters* **2011,** 11, (12), 5471-5476.
18. Ten Cate, S.; Sandeep, C. S. S.; Liu, Y.; Law, M.; Kinge, S.; Houtepen, A. J.; Schins, J. M.; Siebbeles, L. D. A., Generating free charges by carrier multiplication in quantum dots for highly efficient photovoltaics. *Acc Chem Res* **2015,** 48, (2), 174-181.
19. Gao, Y.; Aerts, M.; Sandeep, C. S. S.; Talgorn, E.; Savenije, T. J.; Kinge, S.; Siebbeles, L. D. A.; Houtepen, A. J., Photoconductivity of PbSe quantum-dot solids: Dependence on ligand anchor group and length. *ACS Nano* **2012,** 6, (11), 9606-9614.
20. Liu, Y. G., M.; Puthussery, J.; Gaik, S.; Ihly, R.; Hillhouse, H. W.; Law, M. , Dependence of Carrier Mobility on Nanocrystal Size and Ligand Length in PbSe Nanocrystal Solids. *Nano Lett.* **2010**, (10), 1960-1969.
21. Ihly, R. T., J.; Liu, Y.; Gibbs, M.; Law, M. , The Photothermal Stability of PbS Quantum Dot Solids. *ACS Nano* **2011**, (5), 8175−8186.
22. Liu, Y.; Gibbs, M.; Perkins, C. L.; Tolentino, J.; Zarghami, M. H.; Bustamante, J.; Law, M., Robust, functional nanocrystal solids by infilling with atomic layer deposition. *Nano Letters* **2011,** 11, (12), 5349-5355.
23. Gai, Y.; Peng, H.; Li, J., Electronic properties of nonstoichiometric PbSe quantum dots from first principles. *Journal of Physical Chemistry C* **2009,** 113, (52), 21506-21511.
24. Etgar, L.; Lifshitz, E.; Tannenbaum, R., Hierarchical conjugate structure of γ-Fe2O3 nanoparticles and PbSe quantum dots for biological applications. *Journal of Physical Chemistry C* **2007,** 111, (17), 6238-6244.
25. Liu, Y.; Tolentino, J.; Gibbs, M.; Ihly, R.; Perkins, C. L.; Crawford, N.; Hemminger, J. C.; Law, M., PbSe quantum dot field-effect transistors with air-stable electron mobilities above 7 cm2 V-1 s-1. *Nano Letters* **2013,** 13, (4), 1578-1587.
26. Puurunen, R. L., Surface chemistry of atomic layer deposition: A case study for the trimethylaluminum/water process. *Journal of Applied Physics* **2005,** 97, (12).
27. Miikkulainen, V.; Leskelä, M.; Ritala, M.; Puurunen, R. L., Crystallinity of inorganic films grown by atomic layer deposition: Overview and general trends. *Journal of Applied Physics* **2013,** 113, (2).
28. Suntola, T., Atomic layer epitaxy. *Thin Solid Films* **1992,** 216, (1), 84-89.
29. Beetstra, R.; Lafont, U.; Nijenhuis, J.; Kelder, E. M.; Van Ommen, J. R., Atmospheric pressure process for coating particles using atomic layer deposition. *Chemical Vapor Deposition* **2009,** 15, (7-9), 227-233.
30. Valdesueiro, D.; Meesters, G.; Kreutzer, M.; van Ommen, J., Gas-Phase Deposition of Ultrathin Aluminium Oxide Films on Nanoparticles at Ambient Conditions. *Materials* **2015,** 8, (3), 1249-1263.
31. George, S. M., Atomic layer deposition: An overview. *Chemical Reviews* **2010,** 110, (1), 111-131.
32. Groner, M. D.; Fabreguette, F. H.; Elam, J. W.; George, S. M., Low-Temperature Al2O3 Atomic Layer Deposition. *Chemistry of Materials* **2004,** 16, (4), 639-645.
33. Tripp, M. K.; Stampfer, C.; Miller, D. C.; Helbling, T.; Herrmann, C. F.; Hierold, C.; Gall, K.; George, S. M.; Bright, V. M., The mechanical properties of atomic layer deposited alumina for use in micro- and nano-electromechanical systems. *Sensors and Actuators A: Physical* **2006,** 130–131, (0), 419-429.
34. Lu, P.; Demirkan, K.; Opila, R. L.; Walker, A. V., Room-temperature Chemical Vapor Deposition of Aluminum and Aluminum Oxides on Alkanethiolate Self-Assembled Monolayers. *The Journal of Physical Chemistry C* **2008,** 112, (6), 2091-2098.

35. Zhang, J.; Tolentino, J.; Smith, E. R.; Beard, M. C.; Nozik, A. J.; Law, M.; Johnson, J. C., Carrier transport in PbS and PbSe QD films measured by photoluminescence quenching. *Journal of Physical Chemistry C* **2014,** 118, (29), 16228-16235.
36. Poodt, P.; Lankhorst, A.; Roozeboom, F.; Spee, K.; Maas, D.; Vermeer, A., High-speed spatial atomic-layer deposition of aluminum oxide layers for solar cell passivation. *Advanced Materials* **2010,** 22, (32), 3564-3567.
37. Poodt, P.; Cameron, D. C.; Dickey, E.; George, S. M.; Kuznetsov, V.; Parsons, G. N.; Roozeboom, F.; Sundaram, G.; Vermeer, A., Spatial atomic layer deposition: A route towards further industrialization of atomic layer deposition. *Journal of Vacuum Science & Technology A* **2012,** 30, (1), 010802.
38. Werner, F.; Stals, W.; Görtzen, R.; Veith, B.; Brendel, R.; Schmidt, J. In *High-rate atomic layer deposition of Al2O3 for the surface passivation of Si solar cells*, 1st International Conference on Crystalline Silicon Photovoltaics, SiliconPV 2011, Freiburg, 2011; Freiburg, 2011; pp 301-306.
39. Puurunen, R. L.; Lindblad, M.; Rootc, A.; Krausea, A. O. I., Successive reactions of gaseous trimethylaluminium and ammonia on porous alumina. *Physical Chemistry Chemical Physics* **2001,** 3, (6), 1093-1102.
40. Moreels, I.; Lambert, K.; De Muynck, D.; Vanhaecke, F.; Poelman, D.; Martins, J. C.; Allan, G.; Hens, Z., Composition and Size-Dependent Extinction Coefficient of Colloidal PbSe Quantum Dots. *Chemistry of Materials* **2007,** 19, (25), 6101-6106.
41. Sandeep, C. S. S.; Azpiroz, J. M.; Evers, W. H.; Boehme, S. C.; Moreels, I.; Kinge, S.; Siebbeles, L. D. A.; Infante, I.; Houtepen, A. J., Epitaxially connected PbSe quantum-dot films: Controlled neck formation and optoelectronic properties. *ACS Nano* **2014,** 8, (11), 11499-11511.
42. Barr, T. L.; Seal, S., Nature of the use of adventitious carbon as a binding energy standard. *Journal of Vacuum Science & Technology A* **1995,** 13, (3), 1239-1246.
43. Smith, K. L.; Black, K. M., Characterization of the treated surfaces of silicon alloyed pyrolytic carbon and SiC. *Journal of Vacuum Science & Technology A* **1984,** 2, (2), 744-747.
44. Bastl, Z., X-Ray Photoelectron Spectroscopic Studies of Palladium Dispersed on Carbon Surfaces Modified by Ion Beams and Plasmatic Oxidation. *Collection of Czechoslovak Chemical Communications* **1995**, (60), 383.
45. Gelius, U.; Hedén, P. F.; Hedman, J.; Lindberg, B. J.; Manne, R.; Nordberg, R.; Nordling, C.; Siegbahn, K., Molecular Spectroscopy by Means of ESCA III. Carbon compounds. *Physica Scripta* **1970,** 2, (1-2), 70.
46. Chen, J. J.; Jiang, Z. C.; Zhou, Y.; Chakraborty, B. R.; Winograd, N., Spectroscopic studies of methanol decomposition on Pd[lcub]111[rcub]. *Surface Science* **1995,** 328, (3), 248-262.
47. Solymosi, F.; Berkó, A.; Tóth, Z., Adsorption and dissociation of CH3OH on clean and K-promoted Pd(100) surfaces. *Surface Science* **1993,** 285, (3), 197-208.
48. Hassinen, A.; Moreels, I.; De Nolf, K.; Smet, P. F.; Martins, J. C.; Hens, Z., Short-Chain Alcohols Strip X-Type Ligands and Quench the Luminescence of PbSe and CdSe Quantum Dots, Acetonitrile Does Not. *Journal of the American Chemical Society* **2012,** 134, (51), 20705-20712.
49. Wank, J. R.; George, S. M.; Weimer, A. W., Nanocoating individual cohesive boron nitride particles in a fluidized bed by ALD. *Powder Technology* **2004,** 142, (1), 59-69.
50. Huang, M. T.; Ishida, H., Surface study of hexagonal boron nitride powder by diffuse reflectance Fourier transform infrared spectroscopy. *Surface and Interface Analysis* **2005,** 37, (7), 621-627.

678 51. Ikuno, T.; Sainsbury, T.; Okawa, D.; Fréchet, J. M. J.; Zettl, A., Amine-functionalized
679 boron nitride nanotubes. *Solid State Communications* **2007,** 142, (11), 643-646.
680 52. Li, J.; Xiao, X.; Xu, X.; Lin, J.; Huang, Y.; Xue, Y.; Jin, P.; Zou, J.; Tang, C.,
681 Activated boron nitride as an effective adsorbent for metal ions and organic pollutants. *Sci.*
682 *Rep.* **2013,** 3.
683 53. Igari, S.; Takahisa, K., Accelerated irradiance and temperature cycle test for
684 amorphous silicon photovoltaic devices. *Progress in Photovoltaics: Research and*
685 *Applications* **2014,** 22, (6), 690-696.
686 54. Salameh, S.; Schneider, J.; Laube, J.; Alessandrini, A.; Facci, P.; Seo, J. W.; Ciacchi,
687 L. C.; Mädler, L., Adhesion mechanisms of the contact interface of TiO 2 nanoparticles in
688 films and aggregates. *Langmuir* **2012,** 28, (31), 11457-11464.
689
690

691

692

693 **TABLE OF CONTENTS IMAGE (Graphical abstract)**

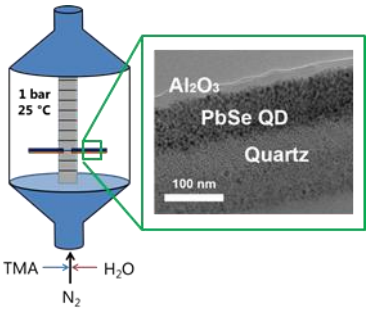

694

695

696

697

698

699

700

701

702